Elsevier Editorial System(tm) for Coastal Engineering
Manuscript Draft

Manuscript Number: CENG-D-15-00010R1

Title: Biophysical properties of salt marsh canopies - Quantifying plant stem flexibility and above ground biomass

Article Type: Research Paper

Keywords: Wave attenuation; Vegetation structure; Drag; Flexural rigidity; Young's bending modulus

Corresponding Author: Ms. Franziska Rupprecht,

Corresponding Author's Institution:

First Author: Franziska Rupprecht

Order of Authors: Franziska Rupprecht; Franziska Rupprecht; Iris Möller; Ben Evans; Tom Spencer; Kai Jensen

Abstract: The three-dimensional structure of salt marsh plant canopies, amongst other marsh surface characteristics, is of critical importance to the functioning and persistence of coastal salt marshes. Together with plant flexibility it controls the contribution of vegetation to the tidal flow and wave energy dissipation potential of marshes. However detailed information on these two key biophysical properties of salt marsh canopies is scarce.
In this paper we present biophysical properties of four plants commonly occurring in NW European salt marshes. We measured stem flexibility, diameter and height of the grasses Spartina anglica, Puccinellia maritima and Elymus athericus and above ground biomass and canopy height in stands of Elymus athericus and the dwarf shrub Atriplex portulacoides. Further we compared the performance of two methods for the non-destructive assessment of above ground biomass, such that they may be used during field assessments of marsh surface vegetation structure (i) Measurement of light availability within the canopy and (ii) side-on photography of vegetation. All data were collected on a salt marsh on the Dengie Peninsula, eastern England, UK, in summer (July).
We found significant differences in stem flexibility both between species and between the different parts of their stems. P. maritima was found to be the species with the most flexible stems, and, as a result of their relatively large stem diameter, S. anglica the species with the stiffest stems. Above ground biomass and hence potential canopy resistance to water flow could be estimated more accurately by side-on photography of vegetation than from measurement of light availability within the canopy.
Our results extend the existing knowledge base on plant properties with relevance to studies of habitat structure and ecosystem functioning as well as wave energy dissipation in salt marsh environments and can be used for the development of a more realistic representation of vegetation in numerical models and laboratory flume studies of plant-flow interactions.

*Highlights (for review)

Highlights

- Paper reports quantitative data on plant flexibility and above ground biomass (a proxy for vegetation structure), in salt marsh canopies. Both these biophysical properties of salt marsh canopies need to feed into flow and wave dissipation models, if the predictive capacity of such models is to be improved.
- Stem flexibility of salt marsh plants differs significantly both between different species and between the different stem parts of specimens of one species.
- Side-on photography of vegetation is an appropriate technique for non-destructive assessment of above ground biomass and vegetation structure in structurally complex salt marsh canopies.
- Above ground biomass and its vertical distribution within the canopy can be estimated more accurately by side-on photography than by measurement of light availability in the canopy.

Manuscript for Coastal Engineering

Biophysical properties of salt marsh canopies - Quantifying plant stem flexibility and above ground biomass

F. Rupprecht[a,c*], I. Möller[b,c], B. Evans[c], T. Spencer[c], K. Jensen[a]

[a] Applied Plant Ecology, Biocenter Klein Flottbek, University of Hamburg, Ohnhorststr. 18, 22609 Hamburg, Germany
[b] Fitzwilliam College, Storey's Way, Cambridge, CB3 0DG, UK
[c] Cambridge Coastal Research Unit, Department of Geography, University of Cambridge, Downing Place, Cambridge, CB2 3EN, UK

[*]Corresponding author. E-mail address: franziska.rupprecht@uni-hamburg.de, Phone: +49 (0)40-42816-272

Abstract

The three-dimensional structure of salt marsh plant canopies, amongst other marsh surface characteristics, is of critical importance to the functioning and persistence of coastal salt marshes. Together with plant flexibility it controls the contribution of vegetation to the tidal flow and wave energy dissipation potential of marshes. However detailed information on these two key biophysical properties of salt marsh canopies is scarce.

In this paper we present biophysical properties of four plants commonly occurring in NW European salt marshes. We measured stem flexibility, diameter and height of the grasses *Spartina anglica*, *Puccinellia maritima* and *Elymus athericus* and above ground biomass and canopy height in stands of *Elymus athericus* and the dwarf shrub *Atriplex portulacoides*. Further we compared the performance of two methods for the non-destructive assessment of above ground biomass, such that they may be used during field assessments of marsh surface vegetation structure (i) Measurement of light availability within the canopy and (ii) side-on photography of vegetation. All data were collected on a salt marsh on the Dengie Peninsula, eastern England, UK, in summer (July).

We found significant differences in stem flexibility both between species and between the different parts of their stems. *P. maritima* was found to be the species with the most flexible stems, and, as a result of their relatively large stem diameter, *S. anglica* the species with the stiffest stems. Above ground biomass and hence potential canopy resistance to water flow could be estimated more accurately by side-on photography of vegetation than from measurement of light availability within the canopy.

Our results extend the existing knowledge base on plant properties with relevance to studies of habitat structure and ecosystem functioning as well as wave energy dissipation in salt marsh environments and can be used for the development of a more realistic representation of vegetation in numerical models and laboratory flume studies of plant-flow interactions.

Key words:

Wave attenuation, vegetation structure, drag, flexural rigidity, Young's bending modulus

1 Introduction

Vegetation is an important factor affecting both the functioning and form of salt marsh ecosystems at the coast. The often structurally complex plant canopies provide a key habitat and food source for a wide range of bird and athropod species as well as contributing to the dissipation of wave energy and tidal flow over salt marsh surfaces directly, via plant-flow interactions, and indirectly, through causing spatially varying sediment accumulation and thus the formation of topographic roughness (Zedler et al. 2005, Gedan et al. 2011; Duarte et al. 2013; Möller et al. 2014). Under wave motion, and when water depths are low enough to allow wave-induced orbital flow to penetrate into the canopy layer, vegetation interacts with this flow by forming an obstruction. In return it experiences drag and re-orientation by wave forces (Mullarney et al. 2010). At the scale of the vegetated landform (e.g. a coastal salt marsh), these plant-flow interactions have been shown to be affected by the spatial configuration of vegetation patches as well as by the ratio of water depth to canopy height (Kirwan and Murray 2007; Vandenbruwaene et al. 2011). At the scale of individual plants, however, the magnitude of flow resistance provided, and drag force experienced, is governed by plant architecture and by mechanical characteristics such as stem flexibility and buoyancy (Paul et al. 2014a).

The flexibility of plant stems, often reported as Young's bending modulus or flexural rigidity (see also section 2.3), is critical for plant behaviour and flow resistance provided under wave-generated orbital flow as well as being a potentially important ecological adaptation mechanism linked to ecosystem resilience. While highly flexible stems bend and take a flattened posture for part of the wave cycle, less flexible stems tend to remain in an upright posture and the flow must travel through, rather than over, the canopy. Peralta et al. (2008) have shown that for a specific range of stem spacings, the capacity of plant canopies to provide flow resistance and dissipate hydrodynamic energy increases with decreasing stem flexibility. A more recent flume study of the salt marsh grasses *Elymus athericus* and *Puccinellia maritima* also highlighted the importance of plant flexibility for wave dissipation during storm surge conditions (2 m water depth above the marsh surface and waves of 40-80 cm in height) (Möller et al. 2014).

While the importance of plant stem flexibility has begun to be recognized through the studies mentioned above, field studies on plant stem flexibility are still scarce and limited to only a few species (see, for example, Feagin et al.'s 2011 study on *Spartina alterniflora*). Laboratory flume studies providing a controlled environment to investigate vegetation-induced flow and wave dissipation often use artificial plant mimics instead of real plants. Quantitative data on plant flexibility can aid to develop more realistic

plant mimics and hence a more realistic representation the interaction between vegetation and hydrodynamics in flume studies.

A realistic representation of the interactions between flow and vegetation is also needed for accurately modelling coastal hydrodynamics. While some models approximate vegetation with higher bottom friction factors (Möller et al. 1999, Augustin et al. 2009), the majority of numerical models capture vegetation effects in a vegetation factor that consists of e.g. plant stem height, stem density and diameter and a empirical bulk drag coefficient C_D (e.g. Kobayashi et al. 1993, Mendez and Losada 2004, Paul et al. 2011, Möller et al. 2014). C_D is a function of both flow regime and plant characteristics and accounts for the ignorance of varying responses of different plant species to hydrodynamic forcing, that means it can be calibrated to different plant architecture or flexibility. The inclusion of a vertical layer schematization for the vegetation as proposed by Suzuki et al. (2011), enables the calibration of C_D for vertical variations in canopy density. In general the value of C_D reflects the flow resistance provided by vegetation, for example canopies composed of flexible plants with low amounts of above ground biomass can be expected to yield lower values of C_D than stiff plants and large amounts of above ground biomass.

Salt marshes present a great diversity in plant architecture and a significant degree of flow resistance might be achieved by branching upper stems and their leaves in addition to the basal stems (Möller and Spencer 2002; Möller 2006; Paul et al. 2014a). As above ground biomass varies with volume and density of plant material present, it can be regarded as a useful proxy for these more complex structural canopy bulk properties, if not necessarily for flexibility and buoyancy. At the scale of plant stands, a positive correlation between canopy density, above ground biomass and wave dissipation has been observed (Koch and Gust 1999, Bouma et al. 2005, Möller 2006). As branches and leaves can constitute a significant proportion of the overall plant above ground biomass (Russell et al. 1990), these non-stem components may contribute significantly to wave dissipation. Canopies with the same total above ground biomass, however, can differ in stem flexibility, buoyancy, canopy architecture and the amount of biomass present at different levels within the canopy. Apart from affecting the canopy's flow- and wave-dissipation capacity above ground biomass and the arrangement of plant elements within the canopy (canopy structure) also play an important role for sediment dynamics and carbon stocks in salt marshes and constitutes an important habitat factor for arthropod and breeding-bird communities (Temmermann et al. 2005, Van Klink et a. 2013, Mandema et al. 2013).

The dependence of a range of ecosystem services (e.g. coastal protection, carbon stocks and habitat provisioning) on a complex set of salt marsh vegetation canopy attributes calls for a critical assessment of methods that can be used to measure not only above ground biomass but also canopy structure, and

the vertical distribution of both, which cannot be captured as such by traditional biomass harvesting methods (Neumeier 2005).

As a method of capturing the more complex structure of vegetation canopies in non-destructive ways, side-on photography of vegetation (Zehm et al. 2003; Möller 2006), hereafter referred to as the photo-method), has been trialled. Observed wave and flow dissipation by simple salt marsh canopies composed of *Salicornia europaea*, *Suaeda maritima* and *Spartina anglica* has been found to reflect variations in both above ground biomass and projected surface area of the canopy as determined by the photo-method (Möller 2006). A difficulty of this methodology is that flow resistance by dense canopies could be underestimated. Beyond a critical threshold value of biomass, plant elements may shade one another and a further increase of biomass may thus no longer be reflected in an increase in the projected surface area. The relationship between projected surface area and biomass, however, has not yet been established for a wider range of canopy densities and for different types of canopy architecture.

Furthermore, there has so far been no comparison between the photo-method and other non-destructive ways of assessing above ground biomass and canopy structure such as the measuring of light availability in the canopy (Schrautzer and Jensen 2006). The light measurement approach originates from the field of agricultural science, where it has been used to estimate crop yields (Webb et al. 2008). In comparison to the photo-method, measurements of light availability offer several advantages. The above ground biomass estimates are derived by analysing a larger surface area and can be calculated directly from the light availability recorded, while the photo-method requires the complex processing of vegetation photographs that can be affected by subjective interpretation (Neumeier 2005). Moreover, damage to the vegetation is minimized as the slim light measuring probe can be easily inserted into even the densest canopies.

In this study we consider plant flexibility and above ground biomass, two biophysical properties of salt marsh canopies that both need to feed into wave dissipation models, if the predictive capacity of such models is to be improved; furthermore we evaluate two methodologies to assess above ground biomass as a proxy for more complex canopy bulk properties such as canopy structure and density:

(i) we present field observations of stem flexibility as well as stem diameter and stem length of *S. anglica*, *Puccinellia maritima* and *E. athericus,* three grasses that form large stands in many salt marshes of NW Europe; and

(ii) we compare the performance of the photo-method with that using measurements of light availability for non-destructive assessment of above ground biomass in canopies of two salt

marsh species with different canopy structure: *Atriplex portulacoides*, a dense low growing dwarf shrub and *E. athericus*, a tall upright growing grass.

Our study thus presents the first data set with systematically collected information on biophysical properties of salt marsh canopies acquired by using a series of alternative methodologies. In this way it provides critical input not only for the study of the ecological importance of canopy structure but also for a greater insight into the reasons why an approximation of hydrodynamic drag based solely on incident flow regime and plant stem density, diameter and height, remains elusive.

2 Methods

2.1 Study site

Field measurements were undertaken in a macro-tidal (MSTR = 4.8 m (Reed 1988)) salt marsh of the UK east coast (Southern North Sea), near Tillingham on the Dengie Peninsula in Essex (Fig.1). The Dengie marshes lie between the estuaries of the Rivers Blackwater and Crouch and form a narrow belt with a maximum of 700 m in marsh width between low lying agricultural land and extensive intertidal mudflats. Over the past 100 – 150 years the marshes have experienced several phases of advance and retreat (Harmsworth and Long 1986; Pye 2000). Marsh surfaces are composed of clayey silts and are approximately horizontal, with elevations of between 2.4 – 2.7 m ODN (Ordnance Datum Newlyn, which approximates to mean sea level; Fig. 1b, 1c). Current rates of relative sea level rise for the Dengie Peninsula have been estimated at 2 - 3 mm a^{-1} (Burningham and French 2011). The vegetation of the Dengie marshes is typical of UK east coast salt marshes (Adam 1988). Marsh edge erosion has all but removed the low marsh communities near Tillingham, but near the seaward marsh edge, plant communities occur at elevations ≤ 2.5 m ODN; Fig. 1b, 1c) and are characterized by *Aster tripolium*, *S. anglica, Suaeda maritima* and pioneer *Salicornia europaea*. Mid to high marsh plant communities occur at elevations > 2.5 m ODN (Fig. 1b, 1c) and are characterized by a canopy of *P. maritima* and *A. portulacoides* with *E. athericus* occurring on levees along creek margins. These species form mixed canopies but also exist in distinct mono-specific patches of several square metres in size, such that approximately uniform vegetation types can be found in close proximity to each other. Over an annual time scale, offshore wave heights have been estimated as averaging 1.09 m (on Long Sand Head, 42 km

NE of Tillingham), while winter (January) mean monthly maxima reach 1.45 – 1.70 m (Herman 1999). Over the vegetated marsh edge (at an elevation of 2.4 m ODN) at Tillingham (Fig. 1b, 1c), water depths have been observed to vary between 0.12 and 0.84 m (mean of 0.43 m) over 236 tidal inundations recorded within one year. For the same tides and time period, significant wave heights were less than 0.87 m on all occasions over the tidal mudflat (Möller and Spencer 2002).

 # Fig. 1

2.2 Species

S. anglica C.E. Hubbard

S. anglica is a perennial grass typically occurring in the pioneer zone and the low marsh (Adam 1993). Throughout the last century, *S. anglica* has spread from its original site (southern coast of UK), both naturally and through deliberate transplantation, to salt marshes all over Europe. The main reason for the planting of *S. anglica* was the perceived stabilization of mudflats as a precursor to land claim or for coastal protection.

P. maritima Huds. Parl.

The perennial grass *P. maritima* has its typical habitat in the low marsh, although at Tillingham, it extends into the mid marsh and in salt marshes with sandy substrates it can also be found in the pioneer zone. *P. maritima* is a common grass of European salt marshes and especially of grazed salt marshes, as the species is tolerant to trampling, biomass loss and waterlogging.

A. portulacoides (L.) [syn. *Halimione portulacoides* Aellen, *Obione portulacoides* (L.) Moq.]

A. portulacoides is a perennial dwarf shrub occurring in European salt marshes, but also in salt marshes along the coasts of North Africa and South-West Asia (Redondo-Gomez et al. 2007). The distribution of *A. portulacoides* within salt marshes depends on soil drainage as the species is lacking aerenchyma and needs aerated substrates. It thus often colonizes creek bank levees on mid- to upper marshes (Cott et al. 2013). In salt marshes of the Wadden Sea on the Eastern fringes of the North Sea *A. portulacoides* often forms monospecific stands in the low marsh. Moreover, the species is sensitive to grazing and trampling.

E. athericus (L.)

The tall grass *E. athericus* occurs in European salt marshes from northern Portugal to southern Denmark and along the southern and south eastern coasts of the British Isles (Veeneklaas et al. 2013). Like *A. portulacoides, E. athericus* needs aerated substrates and is sensitive to grazing. In recent decades *E. athericus* has rapidly colonized mainland salt marshes along the North Sea coast, its expansion being related to the abandonment of grazing, high vertical accretion rates and high marsh age (Rupprecht et al. 2014).

2.3 Measurements of plant stem flexibility

To study plant stem flexibility under bending forces orthogonal to the plant stem, as occurs in vegetation canopies under wave forcing, we conducted three-point-bending tests with bottom, middle and top stem sections of *S. anglica*, *P. maritima* and *E. athericus*. These tests yielded information on Young's bending modulus, *E*, a measure describing how much force has to be applied to bend the stem to a defined displacement. The higher the value for *E*, the less flexible the plant stem. The second moment of area *I* describes the effect of stem morphology (considering stem diameter) on its flexibility. The value of *I* increases with stem diameter. The product of *E* and *I*, known as flexural rigidity, gives a measure of overall stem flexibility. High values of flexural rigidity indicate low stem flexibility.

Samples were collected in the study area in July 2013. For each plant species a small salt marsh section (around 25 cm^2) was excavated, placed in a bucket and transferred to the laboratory. The three-point-bending tests (hereafter referred to as bending tests) were conducted within 14 days of excavating the plants and soil base in the field. Within this time period, plants were kept outside and watered with fresh water.

In total 15 stems of each species were harvested and used for bending tests. Prior to performing the tests, stem length up to the onset of the youngest leaf was measured and stems were divided into three equal parts (bottom, middle, top). The test section was cut from the middle of each part. To minimize the effect of shear stress, a maximum stem-diameter-to-length ratio of 1:15 was chosen. At each end of the stem sections, two diameters were measured with an electronic caliper (precision ± 0.5 mm). Bending tests of *S. anglica* were conducted with a standardized stem section length of 50 mm and, for *P. maritima* and *E. athericus*, a length of 36 mm.

The bending tests were performed with an INSTRON 5544 mechanical testing machine (precision ± 0.5%) using a 100 N load cell (INSTRON Corporation, Canton, MA, USA). The stem test section was placed

centrally onto two support bars and a metal bar was lowered from above at a displacement rate of 10 mm min^{-1} (Fig. 2). The vertical deflection of the stem, *D*, and the corresponding force, *F,* were recorded. Flexural rigidity was calculated from the slope of the force deflection curve *F*/*D* as $EI = (s^3F)/(48D)$, where *s* is the horizontal span of the stem between the two support bars (Fig. 3) (Usherwood et al. 1997).

The second moment of area was calculated as

$$I_c = \pi d^4/64 \qquad [1]$$

for circular cross sections (*S. anglica*, *P. maritima* and *E. athericus*) and as

$$I_{ch} = \pi(d^4_{\text{inner}} - d^4_{\text{outer}})/64 \qquad [2]$$

for circular hollow cross sections (as occurring for some bottom stem sections of *S. anglica*), where *d* = stem diameter (Niklas 1992). From the flexural rigidity, *EI,* and the second moment of area, *I*, the Young's bending modulus, *E*, was calculated as

$$E = EI/I_c = (4\, s^3 F)/3D\Pi\, d^4) \qquad [3]$$

for stem sections with a circular cross section and as

$$E = EI/I_{ch} \qquad [4]$$

for stem sections with a circular hollow cross sections. To analyse the differences in flexural rigidity between species and between stem sections within each species, Kruskall-Wallis tests were performed using R software version 3.1.0 (R Development Core Team, Vienna, AT) as the data did not meet the assumptions required for an Analysis of Variance (ANOVA).

#Fig. 2

 # Fig. 3

2.4 Non-destructive assessment of above ground biomass by the photo-method and by measurements of light availability

Field measurements were undertaken in July 2013. In both stands of *A. portulacoides* (hereafter referred to as *Atriplex*) and *E. athericus* (hereafter referred to as *Elymus*) 10 plots of 1 x 1 m size were chosen to represent a range of various canopy densities. Canopy height was measured at 10 randomly chosen locations within each plot using a folding rule. In the case of *Elymus*, the stem length was recorded whilst for *Atriplex* the height of the youngest leaf or branch tip was measured. At each plot, light availability in the canopy was recorded initially, followed by the application of the photo-method as described below. To calibrate both methods by identifying the relationship between light availability and dry above ground biomass (hereafter referred to as biomass) as well as between canopy density on the photograph and biomass, the vegetation contained in the plot sections used for the photo-method (0.6 m x 0.2 m) was harvested and the dry biomass determined, after drying for 48 h at 60°C.

2.4.1 Measurement of light availability

Light availability in the canopy was recorded by measuring photosynthetically active radiation (PAR) with a Sunscan Canopy Analysis System (Delta T Devices Ltd. Cambridge, UK). The method uses a 0.015 m x 1 m probe containing 64 photodiodes that is inserted into the canopy (Fig. 4a). Light conditions were clouded skies at noon. On each of the 1 m^2 plots five measurements were taken in the *x*- and five in the *z*-dimension of the plot. All measurements were taken on the soil surface above the litter layer. PAR measurements were expressed as relative irradiance (*RI*) which characterizes the light intensity within the canopy relative to that existing above the canopy. PAR above the canopy was measured with a incident solar radiation sensor mounted on a tripod immediately above the canopy. *RI* decreases with increasing canopy density from the top of the canopy towards the soil surface. For a better comparability of *RI* with results of the photo-method, we converted the *RI*-values into values of '*RI absorbed*' (*RIA*) where *RIA* = 100 - *RI*.

#Fig. 4

2.4.2 Photo-method

On each plot a digital photograph of a 0.6 m wide by 0.2 m deep strip of salt marsh vegetation was taken against a red background board using a portable photo-frame (Fig. 4b).

The digital images were processed using Erdas Imagine 10.1 image processing software and a series of programme routines written in Matlab R2012a software to achieve:

1) Rectification and cropping of the image to the size of the background board, thus excluding all other elements besides vegetation and background from the digital photograph (Matlab);

2) Unsupervised classification of each image into 20 classes and subsequent manual class attribution to two classes, yielding binary images with the two classes “vegetation” (0, black pixels) and “background” (1, white pixels). Figure 5 shows a binary picture of the *Atriplex* and the *Elymus* canopy (Erdas Imagine);

3) Further analysis to provide detail on the projected surface area of vegetation expressed as the overall area of vegetation pixels (m^2) per m horizontal image dimension *or vegetation pixel density* (Matlab).

#Fig. 5

2.4.3 Non-destructive assessment of vertical distribution of biomass

In *Elymus* we also applied measurements of light availability and the photo-method to estimate the vertical distribution of biomass within the canopy (hereafter referred to as vertical biomass distribution). Three 1 m^2 plots of *Elymus* similar in canopy density, height (around 0.6 m) and above ground biomass (0.6 ± 0.01 kg/m^2) were chosen. At these plots, light availability was recorded as described in section 2.4.1, on top of the litter layer and at two further canopy heights, 0.2 m and 0.4 m above the litter layer respectively. Subsequently, the photo-method was applied as described in section 2.4.2 three times on each plot. Vegetation pixel density was calculated separately for the vertical canopy layers > 0.4 – 0.6 m (top layer), > 0.2 – 0.4 m (middle layer) and 0 – 0.2 m (bottom layer; 0 m refers to the top of the litter layer, approximately 5 cm above the soil surface). To identify the relationship between light availability and the vertical biomass distribution as well as between vegetation pixel density and vertical biomass distribution, the vegetation contained in the top, middle and bottom canopy layer of the photographed sections of each plot was harvested, transferred to the laboratory, dried for 48 h at 60°C and weighed.

3 Results

3.1 Plant stem flexibility

Measurements of stem length and diameter (Table 1) showed that *S. anglica* and *P. maritim*a were comparable in stem length. The stem length of *E. athericus* exceeded that of *S. anglica* and *P. maritima* by a factor of 2. The stem diameter of *P. maritima* and *E. athericus* was on average around half that of the stem diameter of *S. anglica*.

Flexural rigidity of the three salt marsh grasses under investigation ranged from 0.17 x 10^{-3} Nm^2 (*P. maritima* top stem part) to 3.51 x 10^{-3} Nm^2 (*S. anglica* bottom stem part; Fig. 6, Table 1).

Flexural rigidity was significantly different between all three species (Kruskall-Wallis test, H = 59.33, 2 d.f., $p < 0.01$) and decreased from the bottom to the top of plant stems. In all three species a significant difference was found between the top third and the rest of the stem (Kruskall-Wallis test: *S. anglica*, H = 22.50, 2 d.f. 2, $p < 0.01$; *P. maritima* H = 24.60, 2 d.f. 2, $p < 0.05$; *E. athericus* H = 13.12, 2 d.f. 2, $p < 0.01$).

Values of the Young's bending modulus *E* ranged from 118.28 MPa (*S. anglica* bottom stem part) to 4081.79 MPa (*E. athericus*, bottom stem part; Table 1).

#Table 1

 # Fig. 6

3.2 Assessment of biomass with measurements of light availability and the photo-method

3.2.1 Total biomass

The canopy types under investigation, *Atriplex* and *Elymus*, varied in mean biomass and height. The biomass of *Atriplex* was 1.2 ± 0.5 kg/m^2 with a mean canopy height of 33.1 ± 6.5 cm. Mean biomass of E*lymus* was 0.6 ± 0.2 kg / m^2, corresponding to around half the biomass of *Atriplex* while the canopy height of *Elymu*s (70.8 ± 7.5 cm) exeeded that of *Atriplex* by a factor of 2.

Results from the calibration of measurements of light availability revealed that in both the *Atriplex* and the *Elymus* canopy biomass increased with *RIA* in a non-linear way. A clear relationship between *RIA* and biomass could not be identified. In dense stands of vegetation a further increase of biomass resulted only in minor increases in *RIA* (Fig. 7a, 7b). In the canopy of *Atriplex*, the amount of biomass beyond which no further increase in biomass could be detected (hereafter referred to as biomass threshold value) was well below the mean biomass of *Atriplex,* at around 0.85 kg/m^2. In the *Elymus* canopy, the

biomass threshold value was around 0.68 kg/m^2, close to the mean biomass (0.6 kg/m^2). In both the *Atriplex* and the *Elymus* canopies, values of *RIA* showed high standard deviations (± 5 – 12 %) when biomass was equal or less than 0.6 kg/m^2.

Results from the calibration of the photo-method showed an exponential relationship vegetation pixel density (area of vegetation pixels in m^2 per m horizontal image dimension) and biomass, in the *Atriplex* and *Elymus* canopy, although in *Atriplex* this relationship was somewhat less clear when biomass exceeded 1.0 kg m^{-2} (Fig. 7c, 7d). In both the canopy of *Atriplex* and *Elymus* the biomass threshold value, beyond which a further increase of biomass would no longer result in an increase of vegetation pixel density, does not appear to have been reached in this study.

 # Fig. 7

3.2.2 Vertical biomass distribution

Our results suggest an exponential relationship between *RIA* in the Elymus canopy at heights above the ground of 0.4 m, 0.2 m and on top of the litter layer (0 m) and the amount of biomass in the top canopy layer, the top and the middle canopy layer and of the whole canopy (Fig. 8a). Rates of increase in RIA became smaller with an increase in biomass and conversely with a decrease in height above the ground within the canopy. Measurements of light availability at a defined canopy height represent the cumulative amount of irradiation absorbed by the canopy above. Hence it remains unclear whether this pattern was caused by increase in biomass weight per unit volume or by an increase of canopy density and shading effects.

By contrast the photo-method allowed analysis of vegetation pixel density and biomass in the top, middle and bottom canopy layer alone. We found an exponential relationship between both variables (Fig 8b). This suggests that there was an increase in biomass weight per unit volume with decreasing height within the canopy of *Elymus.*

 # Fig. 8

4 Discussion

4.1 Plant stem flexibility

This study presents the first quantitative data of stem flexibility for the common salt marsh grasses *S. anglica, P. maritima* and *E. athericus,* building on a previous study of a single related species, *Spartina alterniflora* (Feagin et al. 2011). Except for the very flexible species *P. maritima* (with low values of flexural rigidity), the flexural rigidity values of salt marsh grasses recorded in this study were one to four orders of magnitude higher than those described for seagrasses or freshwater plants (Fonseca and Koehl 2006; Miler et al. 2012). Flexural rigidity of bottom and middle stem sections of *S. anglica* and *E. athericus* were within an order of magnitude of flexural rigidity found in stems of brown macroalgae (Paul et al. 2014b).

The fact that flexural rigidity of all three species shows high variability (Fig. 6) may be attributed to differences in the stage of life cycle or vitality of plant stems. Environmental factors as a cause for intraspecific variability may be of minor importance in this study, as all analysed plant stems were harvested from one turf of 25 x 25 cm in size. Very high intraspecific variability of flexural rigidity has also been reported for freshwater plants (Miler et al. 2012) and, independent of sample size, for brown macroalgae (Paul et al. 2014b).

Values of Young's bending modulus, *E*, were much higher than those reported so far for aquatic plants (Table 2). *S. anglica* yielded the smallest values of *E*, in spite of the fact that the species is known for its stiff and upright growing shoots (Bouma et al. 2005). The high values of flexural rigidity which identify *S. anglica* as the stiffest of the considered plant species, result from high values of the second moment of area *I*, i.e. the large stem diameter. This highlights the importance of considering plant size and morphology (here stem diameter) when determining plant biomechanical characteristics (Niklas 1992). For the related species *S. alterniflora*, Feagin et al. (2011) derived values of *E* of 1410 ± 710 MPa which is five to ten times higher than the values reported here for *S. anglica*. However, Feagin et al. (2011) measured *E* with an improvised 3-point-bending test apparatus and, thus their data may not be strictly comparable to the results from this study.

Biophysical properties of salt marsh plants such as stem flexibility, biomass and vegetation density are key parameters controlling their capacity to dissipate wave and tidal flow energy and hence their ability to establish and grow in coastal environments (Bouma et al. 2005; Bouma et al. 2010). Considering stem flexibility alone, *S. anglica*, the species with the strongest and stiffest shoots of all species investigated here, would be expected to be more effective in dissipation of wave energy than species with very thin and flexible stems such as *P. maritima*. Bouma et al. (2010) compared *S. anglica* and *P. maritima* in their ability to dissipate wave energy and found both species to be equally effective due to much higher values for stem density in stands of *P. maritima*. The fact that stem density may

compensate for stiffness illustrates that trade-offs between different biophysical properties needs to be considered when estimating the capacity of marsh surface plant canopies to dissipate wave energy.

Future research should focus on plant movement and breakage in response to various wave conditions as a function of stem flexibility, stem density and biomass. Moreover the values of plant biophysical properties reported here refer to the summer season. Further studies are needed to quantify their seasonal as well as geographical variability.

4.2 Non-destructive assessment of biomass

Our results suggest that the non-destructive assessment of biomass as a proxy for the relative degree of canopy resistance to water flow is possible both with measurements of light availability and the photo-method, albeit with a required species-specific calibration and within set biomass limits. The non-linear relationship between light availability (expressed as percentage of relative irradiation absorbed by the canopy (*RIA*)) and biomass reported here is in accordance with results of Schrautzer and Jensen (2006), who estimated biomass of fen grasslands by measuring light availability. The high standard deviations of light availability in the canopies of *Atriplex* and *Elymus* when biomass was equal or less than 0.6 kg/m^2 suggest that the position of the irradiation measuring probe had a great effect on records of light availability if the canopy density was low. With respect to the photo-method, the clear exponential relationship between projected surface area of vegetation (expressed as vegetation pixel density) and biomass apparent in the *Elymus* canopy, supports the findings of Möller (2006) who estimated biomass with the photo-method at various canopy densities in stands of *S. anglica* (Fig. 7d). In the structurally complex *Atriplex* vegetation type, more samples are needed to verify the exponential increase of biomass with vegetation pixel density (Fig. 7c).

Two main reasons account for the non-linear trend between absorbed relative irradiation and biomass as well as vegetation pixel density and biomass reported here. First, when canopy density increases plant elements in the different horizontal and vertical canopy layers may shade one another, causing saturation in absorbed relative irradiation and in vegetation pixel density. According to our results, measurements of light availability are more sensitive to saturation and an underestimation of biomass due to shading effects than the photo-method.

Second, the space occupied by a plant element in the canopy is not directly related to its weight per volume unit (Neumeier 2005). Consequently, an increase of biomass due to an increase of woody plant elements is not necessarily reflected by a decrease in light availability or an increase in vegetation pixel

density. This applies particularly to assessments of the vertical biomass distribution in the canopy, as in stands of many plant species the percentage of woody plant elements increases near the soil surface.

Our results suggest that the photo-method is more appropriate to assess the vertical distribution of biomass in the canopy than measurements of light availability at different heights within the canopy. Light availability recorded at a defined height within the canopy represents the cumulative absorption of relative irradiation by the canopy layers above. Light penetration from one canopy layer through to the next is strongly affected by variation in spatial arrangement and orientation of plant elements within the canopy. Consequently, it is difficult to establish a relationship between the amount of irradiation absorbed by the top, middle and bottom canopy layer alone and the biomass present in the respective layers.

By contrast, the photo-method allowed for the analysis of vegetation pixel density and biomass in the bottom, middle and top canopy layer. The increase in biomass weight per unit volume with decreasing height in the canopy found in this study implies an increase of lignifications and stiffness of *Elymus* stems near the soil surface – an assumption that is confirmed by the results of the stem flexibility measurements reported in this paper.

Future studies that aim to quantify vegetation canopy resistance to water flow must also address the complication that arises when the submergence of the canopy results in a vertical biomass distribution within the canopy that differs from that measured when the canopy is dry. Once again, the need to consider such canopy buoyancy effects may be species specific, with stiff and upright growing species, such as *Spartina* spp., being less affected than species with more flexible stems, such as *Puccinellia* spp. or *Elymus* spp..

5 Conclusions

This study is the first to provide systematically acquired information on biophysical properties with application to wave dissipation of four typical plant species of NW European salt marshes. It is also the first to compare the performance of two methods for the non-destructive assessment of biomass in salt marshes. Our results show significant differences in stem flexibility, both between different species and between the different stem parts of specimens of one species. This underlines the fact that biomechanical properties often vary not only between, but also within, the individuals of a plant species (Feagin et al. 2011; Miler et al. 2012; Paul et al. 2014a). Flexibility of plant stems and its vertical

distribution affects the bending angle and re-orientation of stems under wave forcing (Feagin et al. 2011).

The comparison of methods for the non-destructive assessment of biomass and canopy structure showed that the photo-method is a more appropriate technique than the measurement of light availability. While measurements of light availability showed saturation at low biomass values, analysis of digital photographs of vegetation allowed for the estimation of biomass over the whole range of biomass values and in both types of canopy architecture tested. Moreover, it was more suitable for the estimation of vertical biomass distribution and, given that it measures the area of the vegetation elements projected into horizontal flow (rather than obstruction to light coming from above), could be considered a more meaningful parameter in relation to flow and wave dissipation.

Our study suggests a way forward for the measurement/quantification of biophysical properties of salt marsh canopies with high relevance to studies of habitat structure and ecosystem functioning as well as flow and wave energy dissipation in salt marsh environments. Considering the application of our findings in numerical models dealing with the interaction between flow and vegetation, data on canopy biomass and structure as well as plant flexibility should now be combined with measurements of flow regime and wave dissipation, to investigate whether it is possible to quantify the currently empirically derived relationship between flow regime, plant spacing (height and diameter), drag, and wave dissipation, a priori. This would mean that models for wave dissipation over such structurally complex canopies could be applied without the requirement for empirical calibration of drag against observed dissipation.

Acknowledgements

This study was carried out with the financial support of the German Academic Exchange Service (DAAD; grant number D/12/44810), while the first author was a visitor at the Cambridge Coastal Research Unit, University of Cambridge. We thank Dr. Michelle Oyen, Anne Bahnweg, Len Howlett and Alan Heaver, Department of Engineering, University of Cambridge, for advice and assistance provided in the measurements of plant stem flexibility.

References

Adam, P. 1988. Geographical variation in British salt marsh vegetation. *J. Ecol.* 66:339–366.

Adam, P. 1993. *Saltmarsh ecology*, Cambridge University Press, Cambridge, UK.

Augustin, L. N., Irish, J. L., Lynett, P. 2009. Laboratory and numerical studies of wave damping by emergent and near-emergent wetland vegetation. *Coast. Eng.* 56:332–340.

Bouma, T. J., De Vries, M. B., Herman, P. M. J. 2010. Comparing ecosystem engineering efficiency of two plant species with contrasting growth strategies. *Ecology* 91:2696–2704.

Bouma, T. J., De Vries, M. B., Low, E., Peralta, G., Tanczos, C., Van De Koppel, J., Herman, P. M. J. 2005. Trade-offs related to ecosystem engineering: A case study on stiffness of emerging macrophytes. *Ecology* 86:2187–2199.

Burningham, H., French, J. 2011. Seabed dynamics in a lage coastal embayment: 180 years of morphological change in the outer Thames estuary. *Hydrobiologia* 672:105–119.

Cott, G. M., Reidy, D. T., Chapman, D. V., Jansen, M. A. K. 2013. Waterlogging affects the distribution of the saltmarsh plant *Atriplex portulacoides* (L.) Aellen. *Flora* 208:336–342.

Duarte, C. M., Losada, I. J., Hendriks, I. E., Mazarrasa, I., Marbà, N. 2013. The role of coastal plant communities for climate change mitigation and adaptation. *Nat. Clim. Change* 3:961–968.

Feagin, R. A., Irish, J. L., Möller, I., Williams, A. M., Colon-Rivera, R. J., Mousavi, M. E. 2011. Short communication: Engineering properties of wetland plants with application to wave attenuation. *Coast. Eng.* 58:251–255.

Fonseca, M. S., Koehl, M. A. R. 2006. Flow in seagrass canopies: The influence of patch width. *Estuar. Coast. Shelf S.* 67:1–9.

Gedan, K. B., Kirwan, M. L., Wolanski, E., Barbier, E. B., Silliman, B. R. 2011. The present and future role of coastal wetland vegetation in protecting shorelines: answering recent challenges to the paradigm. *Climatic Change* 106:7–29.

Harmsworth, G. C., Long, S. P. 1986. An assessment of salt-marsh erosion in Essex, England, with reference to the Dengie Peninsula. *Biol. Conserv.* 35:377–387.

Herman, W. M. 1999. *Wave dynamics in a macro-tidal estuary*. Unpubl. PhD thesis, University of Cambridge, Cambridge, UK.

Kirwan, M. L., Murray, A. B. 2007. A coupled geomorphic and ecological model of tidal marsh evolution. *Proc. Natl. Acad. Sci. U. S. A.* 104:6118–6122.

Kobayashi, N., Raichle, A. W., Asano, T. 1993. Wave attenuation by vegetation. *J. Waterw. Port Coast. Ocean Eng.* 119:30–48.

Koch, E. W., Gust, G. 1999. Water flow in tide- and wave-dominated beds of the seagrass Thalassia testudinum. *Mar. Ecol-Prog. Ser.* 63–72.

Mandema, F. S., Tinbergen, J. M., Ens, B. J., Bakker, J. P. 2013. Spatial diversity in canopy height at Redshank and Oystercatcher nest-sites in relation to livestock grazing. *Ardea* 101:105–112.

Mendez, F. J., Losada, I. J. 2004. An empirical model to estimate the propagation of random breaking and nonbreaking waves over vegetation fields. *Coast. Eng.* 51:103–118.

Miler, O., Albayrak, I., Nikora, V., O'Hare, M. 2012. Biomechanical properties of aquatic plants and their effects on plant-flow interactions in streams and rivers. *Aquat. Sci.* 74:31–44.

Möller, I. 2006. Quantifying saltmarsh vegetation and its effect on wave height dissipation: Results from a UK East coast saltmarsh. *Estuar. Coast. Shelf S.* 69:337–351.

Möller, I., Kudella, M., Rupprecht, F., Spencer, T., Paul, M., Van Wesenbeeck, B. K., Wolters, G., Jensen, K., Bouma, T. J., Miranda-Lange, M., Schimmels, S. 2014. Wave attenuation over coastal salt marshes under storm surge conditions. *Nat. Geosci.* 7: 727–731.

Möller, I., Spencer, T. 2002. Wave dissipation over macro-tidal saltmarshes: Effects of marsh edge typology and vegetation change. *J. Coastal Res.* SI36:506–521.

Möller, I., Spencer, T., French, J. R., Leggett, D. J., Dixon, M. 1999. Wave transformation over salt marshes: A field and numerical modelling study from north Norfolk, England. *Estuar. Coast. Shelf S.* 49:411–426.

Mullarney, J. C., Henderson, S. M. 2010. Wave-forced motion of submerged single-stem vegetation. *J. Geophys. Res. 115*(C12), C12061. doi:10.1029/2010JC006448.

Neumeier, U. 2005. Quantification of vertical density variations of salt-marsh vegetation. *Estuar. Coast. Shelf S.* 63:489–496.

Niklas, K. J. 1992. *Plant biomechanics*, University of Chicago Press, Chicago, USA.

Paul, M., Amos, C. L. 2011. Spatial and seasonal variation in wave attenuation over Zostera noltii. *J. Geophys. Res-Oceans* 116:C08019.

Paul, M., Thomas, R. E., Dijkstra, J. T., Penning, W. E., Vousdoukas, M. I. 2014a. Plants, hydraulics and sediment dynamics. In: Frostick L. E., Thomas R. E., Johnson M. F., Rice S. P., McLelland S. J. (eds.) *Users Guide to Ecohydaulic Modelling and Experimentation: Experience of the Ecohydraulic Research Team (PICES) of the HYDRALAB network*, CRC Press/Balkema, Leiden, NL.

Paul, M., Henry, P.-Y. T. & Thomas, R. E. 2014b. Geometrical and mechanical properties of four species of northern European brown macroalgae. *Coast. Eng.* 84:73–80.

Peralta, G., van Duren, L. A., Morris, E. P., Bouma, T. J. 2008. Consequences of shoot density and stiffness for ecosystem engineering by benthic macrophytes in flow dominated areas: a hydrodynamic flume study. *Mar. Ecol. Prog. Ser.* 368:103–115

Pye, K. 2000. Saltmarsh erosion in southeast England: mechanisms, causes and implications. In: Sherwood B. R., Gardiner, B.G., Harris, T. (eds.) *British salt marshes*, Forrest Text/Linnean Society of London, Cardigan/Cambridge, pp. 359–396.

Redondo-Gomez, S., Mateos-Naranjo, E., Davy, A. J., Fernandez-Munoz, F., Castellanos, E. M., Luque, T., Figueroa, M. E. 2007. Growth and photosynthetic responses to salinity of the salt-marsh shrub *Atriplex portulacoides*. *Ann. Bot-London* 100:555–563.

Reed, D. J. 1988. Sediment dynamics and deposition in a retreating coastal salt-sarsh. *Estuar. Coast. Shelf S.* 26:67–79.

Rupprecht, F., Wanner, A., Stock, M., Jensen, K. 2014. Succession in salt marshes – large-scale and long-term patterns after abandonment of grazing and drainage. *Appl. Veg. Sci*.DOI: 10.1111/avsc.12126.

Russel G., Marshall B., Jarvis P. G. 1990. *Plant canopies: their growth, form and function*. Cambridge University Press, Cambridge, UK.

Schrautzer, J., Jensen, K. 2006. Relationship between fight availability and species richness during fen grassland succession. *Nord. J. Bot.* 24:341–353.

Suzuki, T., Zijlema, M., Burger, B., Meijer, M. C., Narayan, S. 2011. Wave dissipation by vegetation with layer schematization in SWAN. *Coast. Eng.* 59:64–71.

Temmerman, S., Bouma, T. J., Govers, G., Wang, Z. B., De Vries, M. B., Herman, P. M. J. 2005. Impact of vegetation on flow routing and sedimentation patterns: Three-dimensional modeling for a tidal marsh. *J. Geophys. Res-Earth.* 110:F04019.

Usherwood, J. R., Ennos, A. R., Ball, D. J. 1997. Mechanical and anatomical adaptations in terrestrial and aquatic buttercups to their respective environments. *J. Exp. Bot.* 48:1469–1475.

Vandenbruwaene, W., Temmerman, S., Bouma, T. J., Klaassen, P. C., De Vries, M. B., Callaghan, D. P., Van Steeg, P., Dekker, F., Van Duren, L. A., Martini, E., Balke, T., Biermans, G., Schoelynck, J., Meire, P. 2011. Flow interaction with dynamic vegetation patches: Implications for biogeomorphic evolution of a tidal landscape. *J. Geophys. Res.* 116: F01008, doi:10.1029/2010JF001788.

Van Klink, R., Rickert, C., Vermeulen, R., Vorst, O., WallisDeVries, M. F., Bakker, J. P. 2013. Grazed vegetation mosaics do not maximize arthropod diversity: Evidence from salt marshes. *Biol. Conserv.* 164:150–157.

Veeneklaas, R. M., Dijkema, K. S., Hecker, N., Bakker, J. P. 2013. Spatio-temporal dynamics of the invasive plant species *Elytrigia atherica* on natural salt marshes. *Appl. Veg. Sci.* 16:205–216.

Webb, N., Nichol, C., Wood, J., Potter, E. 2008. *User Manual for the SunScan Canopy Analysis System type SS1*, Delta-T Devices Ltd, Cambridge, UK.

Zedler, J. B., Kercher, S. 2005. Wetland resources: status, trends, ecosystem services, and restorability. *Annu. Rev. Environ. Resour.* 30:39–74.

Zehm, A., Nobis, M., Schwabe, A. 2003. Multiparameter analysis of vertical vegetation structure based on digital image processing. *Flora* 198:142–160.

Figure and Table captions

Fig. 1. Study site at the Dengie marshes, Essex, England, UK. Along the transect from X (sea defenceboundary) to Y (intertidal mudflat) across the marsh platform mid marsh plant communities occur at elevations > 2.4 m ODN (Ordnance Datum Newlyn, which approximates mean sea level) and low marsh and pioneer plant communities at elevations ≤ 2.4 m ODN.

Fig. 2. Three-point-bending test apparatus and bending test of a stem section of *Elymus athericus*.

Fig. 3. Force-displacement curve (solid line) from a middle part of a stem of *Elymus athericus.* Young's bending modulus and flexural rigidity were calculated from the slope of the initial linear part (dotted line). The curve shape is representative for all species and stem parts in this study.

Fig. 4. a) Sun scan canopy analysis system used to measure light availability in and above the canopy; b) portable digital photograph frame used to capture side-on photographs of salt marsh vegetation.

Fig 5. Classified binary black and white digital images of the canopy of a) *Atriplex portulacoides* and b) *Elymus athericus* used to estimate above ground biomass from vegetation pixel density from side-on photographs of vegetation.

Fig. 6: Median and variability in flexural rigidity for bottom (Bo), middle (Mi) and top (To) stem parts of three salt marsh grasses. The bottom and top of the box represent the first and third quartiles, ends of whiskers represent the minimum and maximum values. Flexural rigidity was significantly different between all species (Kruskall-Wallis-test, $H = 59.33$, $p < 0.01$, d.f. = 2). Significant differences in flexural rigidity between bottom (Bo), middle (Mi) and top (To) stem parts of *S. anglica*, *P. maritima* and *E. athericus* are marked with A and B.

Fig. 7: Relationship between light availability (expressed as mean ± 1 SD of relative irradiance absorbed by the canopy) in the canopy of a) *Atriplex* and b) *Elymus* and above ground biomass (dry weight), the horizontal black line indicates the threshold beyond which a further increase of biomass did not result in an increase of irradiance absorbed. Relationship between density of vegetation pixels as derived from side-on photography of vegetation in stands of c) *Atriplex* and d) *Elymus* and above ground biomass (dry weight).

Fig 8. Assessment of vertical biomass distribution in the canopy of *Elymus*. a) Relationship between light availability (expressed as relative irradiance absorbed by the canopy) at heights of 0.4 m (top canopy layer), 0.2 m (top and middle canopy layer) and 0 m (whole canopy) and the cumulative amount of above ground biomass present at the corresponding canopy heights. b) Relationship between vegetation pixel density derived from the analysis of side-on photographs for the top (> 0.4 m– 0.6 m), the middle > 0.2 – 0.4 m) and the bottom canopy layer (0 – 0.2 m) and biomass of the respective canopy layers. All values represent mean ± 1 SD from measurements on three plots with a similar amount of above ground biomass (0.6 ± 0.01 kg/m^2).

Table 1. Mean values (±1 standard deviation) for biomechanical properties of three salt marsh grasses.

Table 2. Young's bending modulus and flexural rigidity (mean ±1 standard deviation) of selected species from seagrass, brown macroalgae, freshwater and salt marsh plants.

Table 1. Mean values (±1 standard deviation) for biomechanical properties of three salt marsh grasses.

	Stem diameter [cm]	Stem length [cm]	Flexural rigidity [$x10^{-3}$ Nm^2]	Young's bending modulus [MPa]	Sample size n
S. anglica		27.87 ± 4.66			15
Bottom	0.45 ± 0.06		3.51 ± 0.58	118.28 ± 49.94	15
Middle	0.48 ± 0.05		3.29 ± 1.14	122.90 ± 36.05	15
Top	0.23 ± 0.07		0.69 ± 1.10	310.86 ± 136.93	15
P. maritima		23.93 ± 6.94			15
Bottom	0.14 ± 0.01		0.40 ± 0.14	1995.35 ± 648.70	15
Middle	0.15 ± 0.02		0.45 ± 0.17	1764.90 ± 354.44	15
Top	0.15 ± 0.02		0.17 ± 0.07	736.54 ± 280.60	15
E. athericus		46.00 ± 12.30			15
Bottom	0.16 ± 0.02		1.23 ± 0.64	4081.79 ± 1386.30	15
Middle	0.17 ± 0.02		1.01 ± 0.42	2755.09 ± 694.03	15
Top	0.16 ± 0.02		0.61 ± 0.32	1952.07 ± 667.63	15

Table 2. Young's bending modulus and flexural rigidity (mean ±1 standard deviation) of selected species from seagrass, brown macroalgae, freshwater and salt marsh plants.

	Flexural rigidity [$x10^{-3}$ Nm^2]	Young's bending modulus [MPa]	Source
Seagrass			
Zostera marina	0.00018		Fonseca et al. 2006
Brown macro algae (stems)			
Aliaria esculenta	2.46 ± 0.62	16 ± 4	Paul et al. 2014b
Fucus serratus	2.89 ± 0.89	11 ± 4	Paul et al. 2014b
Laminaria digitata	1.95 ± 0.70	29 ± 13	Paul et al. 2014b
Freshwater plants			
Glyceria fluitans	0.68 ± 0.27	90 ± 33	Miler et al. 2012
Myriophyllum alternifolium	0.025 ± 0.11	89 ± 38	Miler et al. 2012
Ranunculus penicillatus	0.022 ± 0.14	12 ± 7	Miler et al. 2012
Salt marsh plants			
Spartina alterniflora		1410 ± 710	Feagin et al. 2011

Figure 1

Click here to download high resolution image

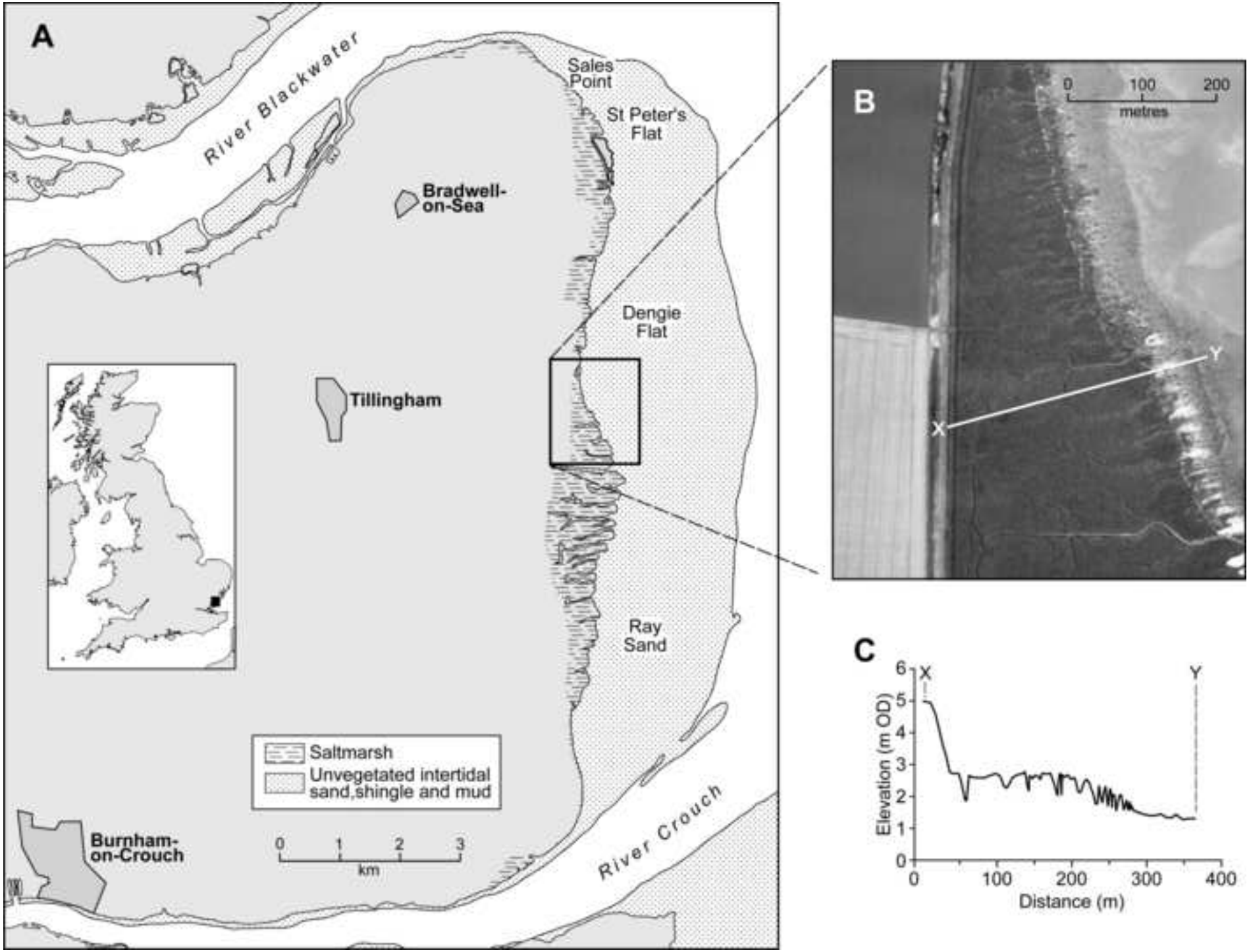

Figure 2
Click here to download high resolution image

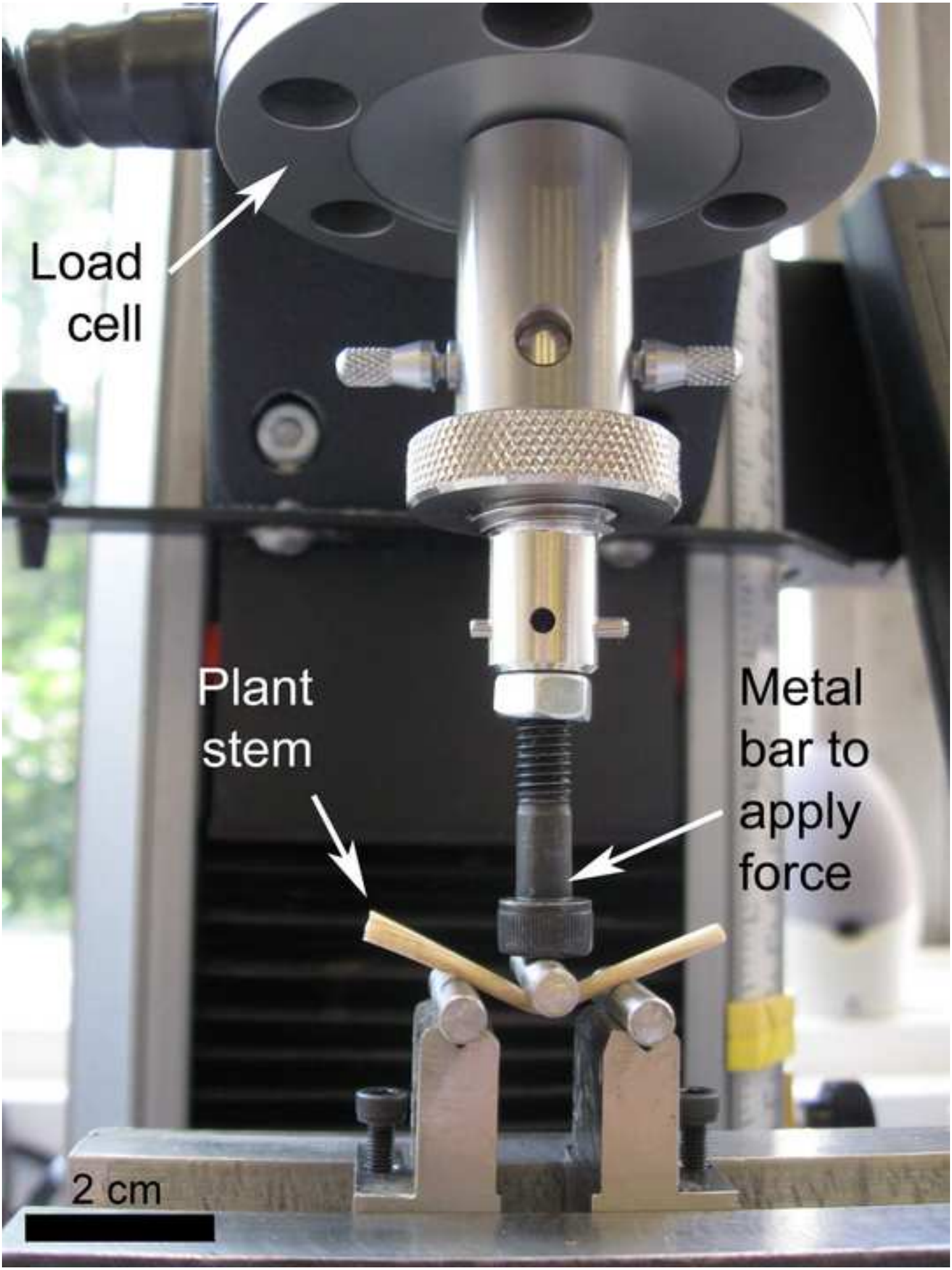

Figure 3

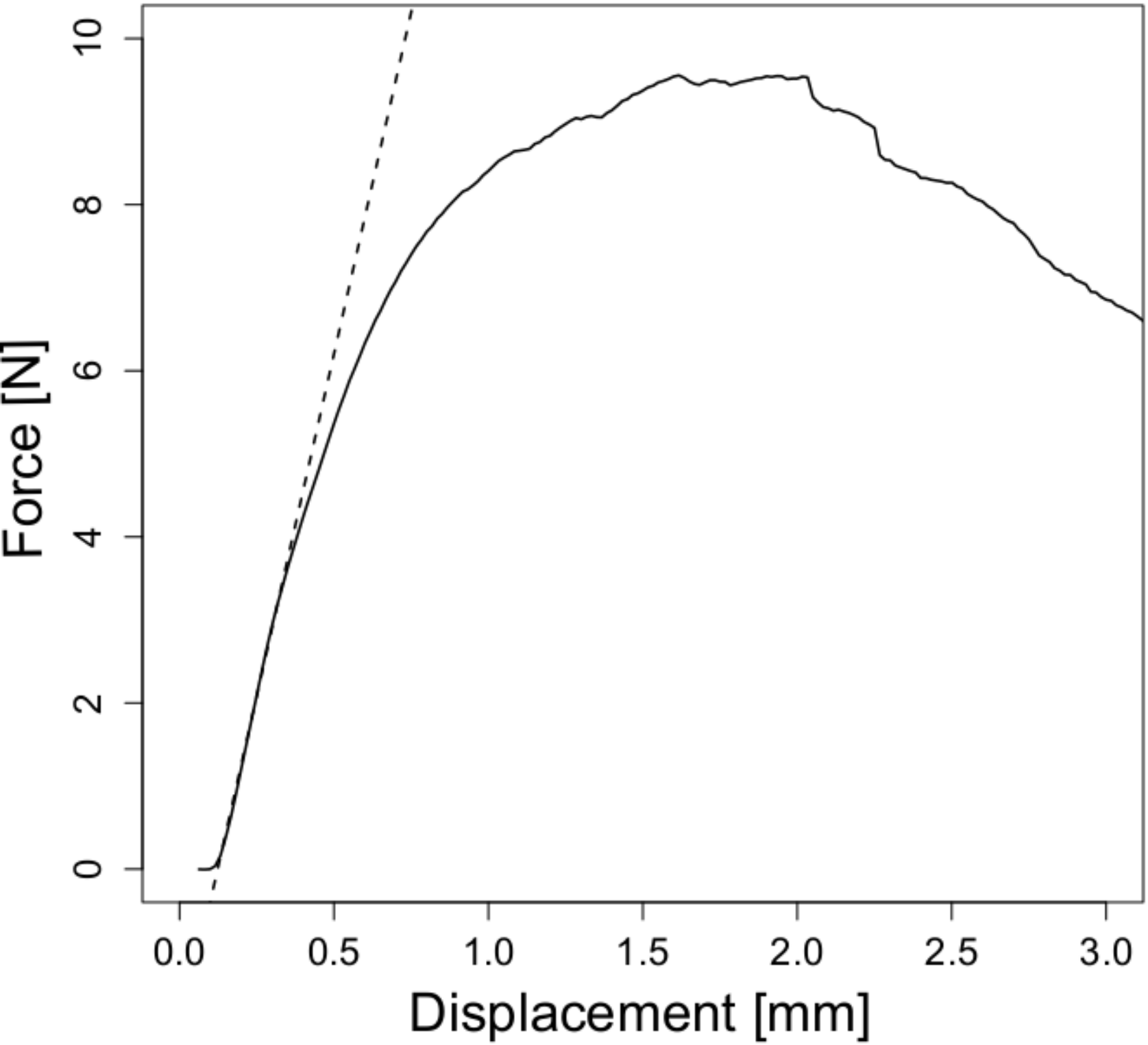

Figure 4

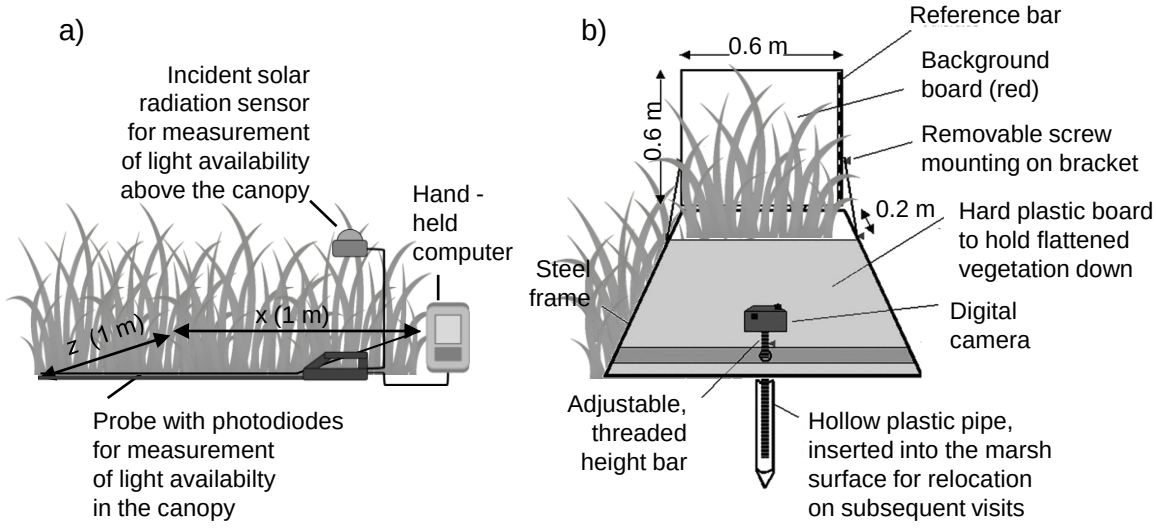
a)
Incident solar radiation sensor for measurement of light availability above the canopy
Hand - held computer
x (1 m)
z (1 m)
Probe with photodiodes for measurement of light availabilty in the canopy
b)
0.6 m
0.6 m
Reference bar
Background board (red)
Removable screw mounting on bracket
0.2 m
Hard plastic board to hold flattened vegetation down
Steel frame
Digital camera
Adjustable, threaded height bar
Hollow plastic pipe, inserted into the marsh surface for relocation on subsequent visits

Figure 5

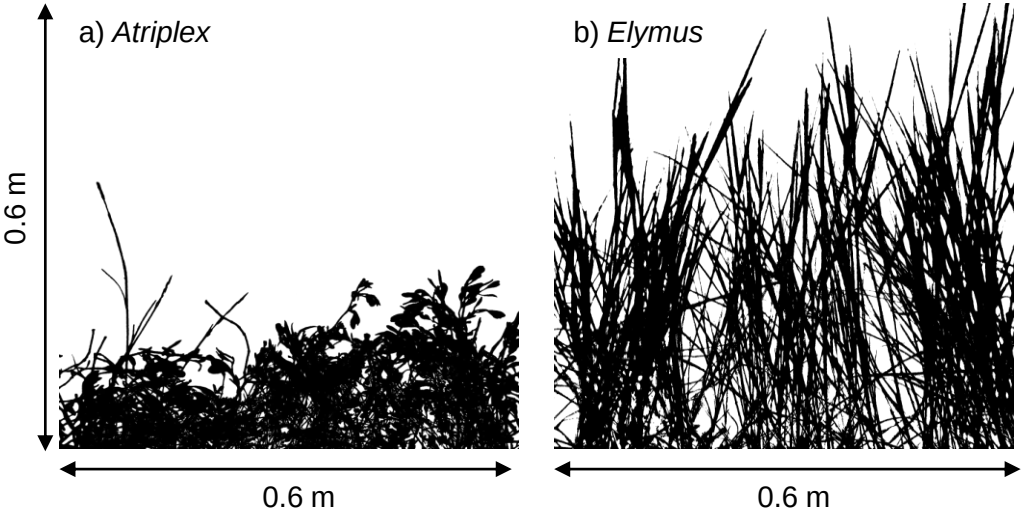

Figure 6

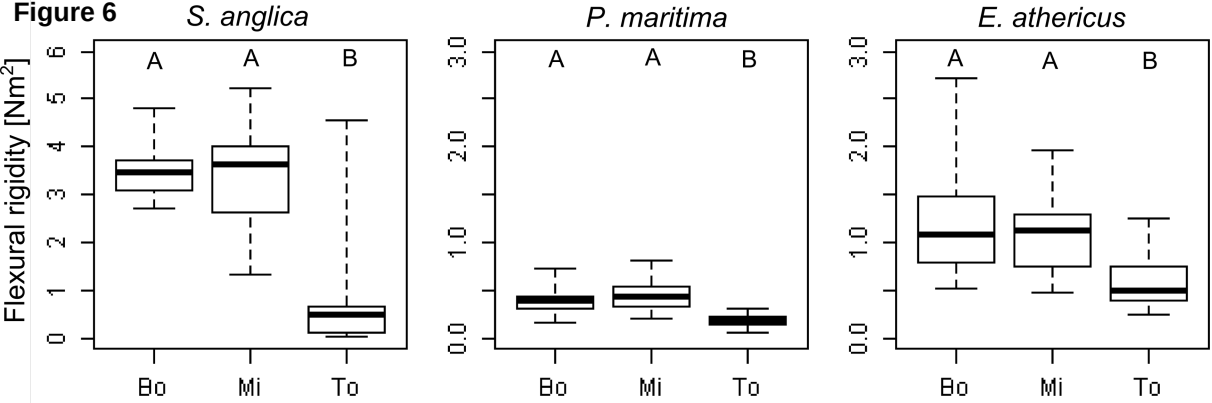
S. anglica
P. maritima
E. athericus
Flexural rigidity [Nm²]
0
1
2
3
4
5
6
0.0
1.0
2.0
3.0
A
A
B
Bo
Mi
To

Figure 7

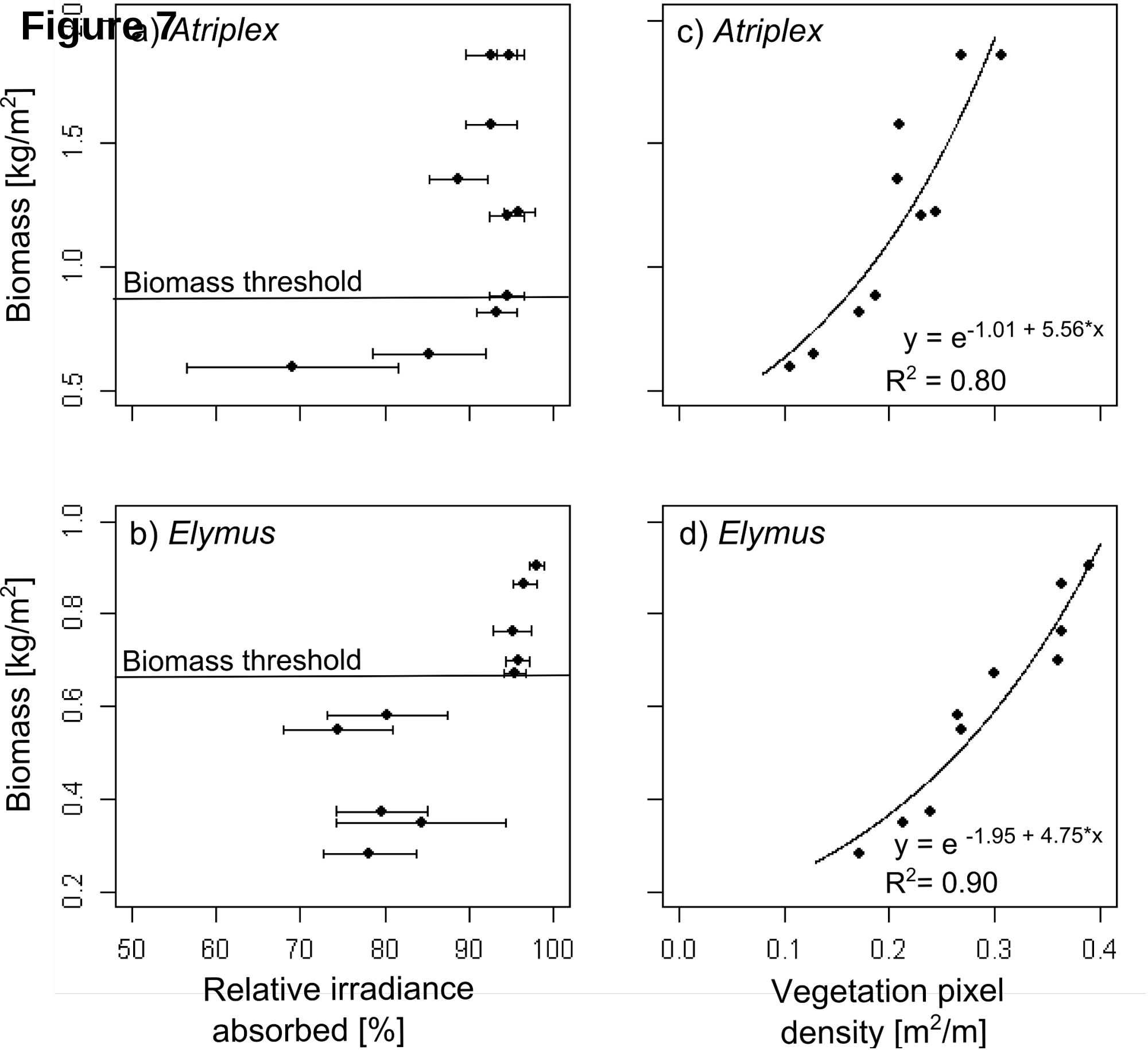
a) Atriplex
Biomass threshold
Biomass [kg/m2]
0.5
1.0
1.5
c) Atriplex
y = e-1.01 + 5.56*x
R2 = 0.80
b) Elymus
Biomass threshold
Biomass [kg/m2]
0.2
0.4
0.6
0.8
1.0
d) Elymus
y = e -1.95 + 4.75*x
R2= 0.90
50
60
70
80
90
100
Relative irradiance absorbed [%]
0.0
0.1
0.2
0.3
0.4
Vegetation pixel density [m2/m]

Figure 8a

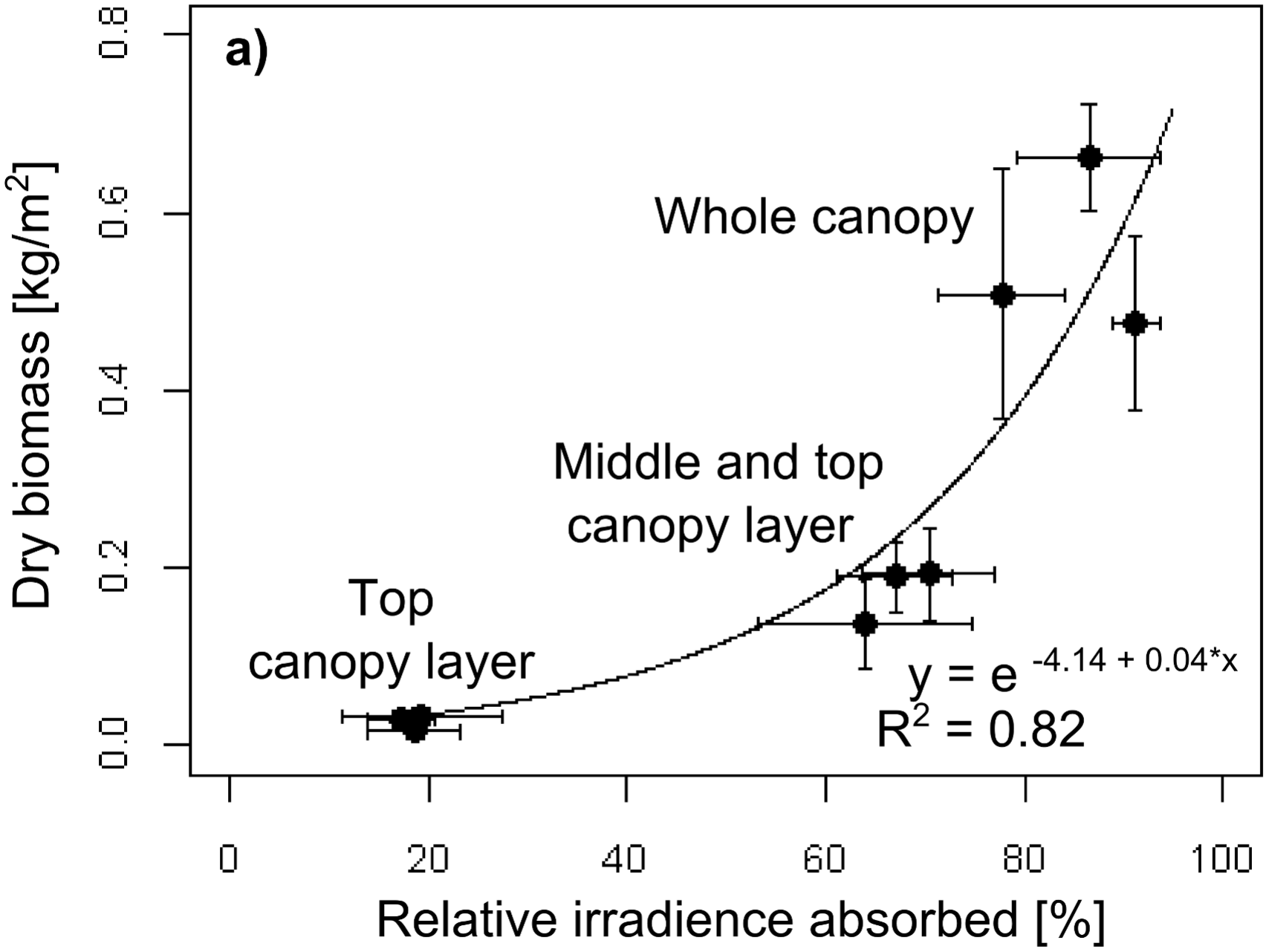
a)
Whole canopy
Middle and top
canopy layer
Top
canopy layer
y = e -4.14 + 0.04*x
R2 = 0.82
Dry biomass [kg/m2]
0.0
0.2
0.4
0.6
0.8
0
20
40
60
80
100
Relative irradiance absorbed [%]

Figure 8b

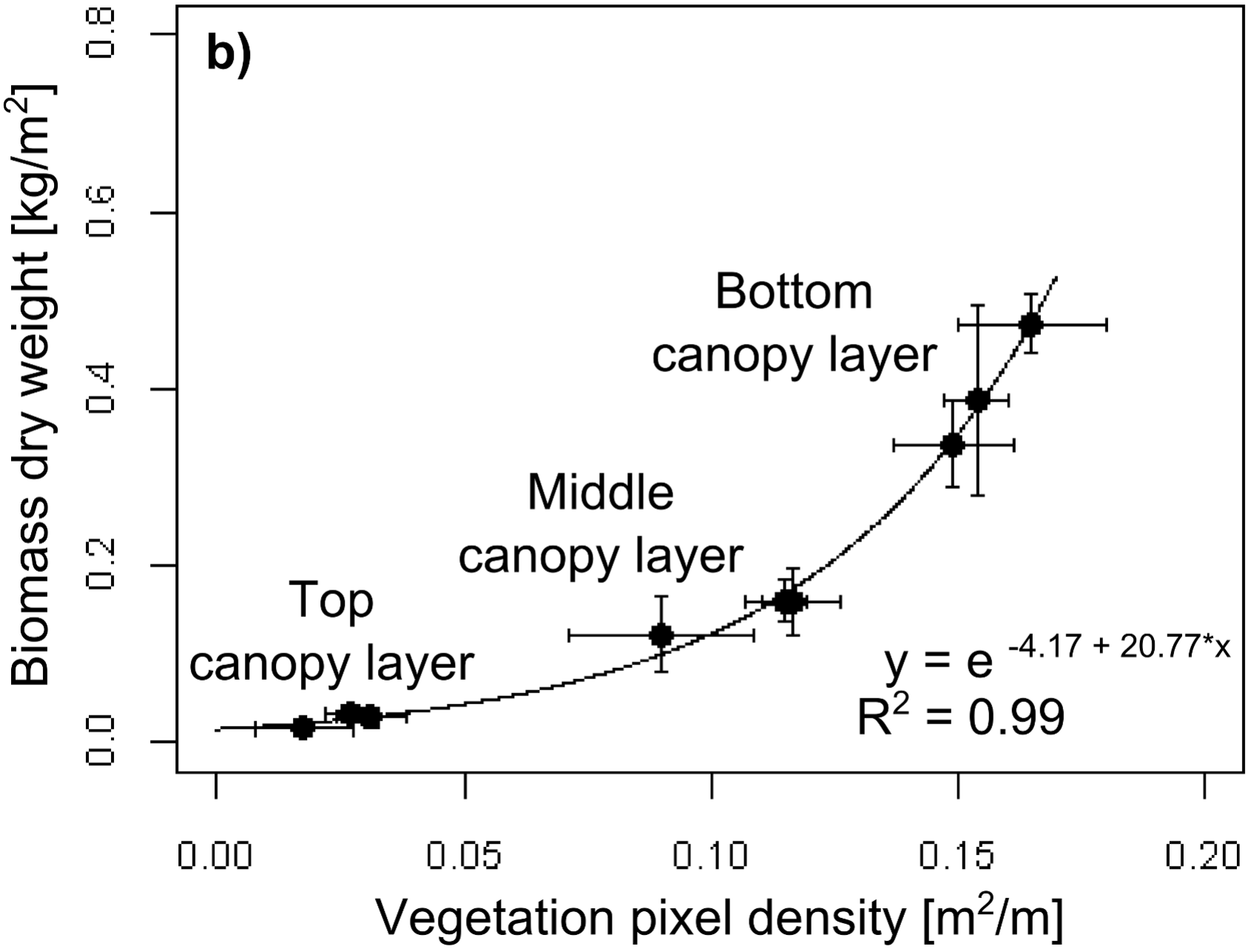
b)
Biomass dry weight [kg/m2]
0.0
0.2
0.4
0.6
0.8
Bottom
canopy layer
Middle
canopy layer
Top
canopy layer
y = e -4.17 + 20.77*x
R2 = 0.99
0.00
0.05
0.10
0.15
0.20
Vegetation pixel density [m2/m]